Acta Polytechnica CTU Proceedings **50**:74–80, 2024
https://doi.org/10.14311/APP.2024.50.0074
© 2024 The Author(s). Licensed under a CC-BY 4.0 licence
Published by the Czech Technical University in Prague

UNDERSTANDING INTRINSIC STRESS EFFECTS ON VIBRATIONAL RESPONSE OF SILICON NANOWIRES

Sina Zare Pakzad[a, b, c], Muhammad Muzammil[d], Mehdi Bostan Shirin[a], Basit Ali[a], Semih Berk Coban[a], Ege Nacarkucuk[a], Umut Kerimzade[a, e], Burhanettin Erdem Alaca[a, e, f, *]

[a] *Koç University, Department of Mechanical Engineering, 34450 Istanbul, Turkey*
[b] *Technische Universität Wien, Institute of Sensor and Actuator Systems, Gusshausstrasse 27-29, 1040 Vienna, Austria*
[c] *Technische Universität Wien, Institute of Sensor and Actuator Systems, Christian Doppler Laboratory for Piezoelectric Silicon MEMS with Enhanced Sensitivity and Responsivity, A-1040 Vienna, Austria*
[d] *Koç University, Computational Sciences and Engineering Program, 34450 Istanbul, Turkey*
[e] *Koç University, n²STAR-Koç University Nanofabrication and Nanocharacterization Center for Scientific and Technological Advanced Research, 34450 Istanbul, Turkey*
[f] *Koç University, Surface Technologies Research Center (KUYTAM), 34450 Istanbul, Turkey*
[*] corresponding author: ealaca@ku.edu.tr

Abstract. Silicon nanowires have become integral components in nanoelectromechanical systems and nanoelectronics. This article explores the intricate relationship between intrinsic stress and mechanical behavior in silicon nanowires. Utilizing a comprehensive approach involving Raman characterization, resonance testing, and thermal processing, the study investigates the induced intrinsic stresses within silicon nanowires. The findings reveal the introduction of 1.4 GPa of intrinsic stress and a 1.3 MHz frequency shift to silicon nanowire through thermal processing. These results underscore the importance of understanding and utilizing intrinsic stresses in silicon nanowires for the advancement of next-generation nanoelectromechanical systems. Overall, this article contributes to the ongoing efforts aimed at fully realizing the potential of silicon nanowires in various scientific and technological domains.

Keywords: Silicon, nanowire, resonance testing, Raman characterization, intrinsic stress.

1. Introduction

Silicon Nanowires (Si NWs) serve as fundamental components in the integration of microelectromechanical systems (MEMS) and nanoelectromechanical systems (NEMS), playing a pivotal role in next-generation electronics, energy applications, and ultra-sensitive sensors [1–3]. With their unique properties and the inherent piezoresistivity, Si NWs exhibit remarkable potential across various domains, bridging fundamental scientific exploration with potential industrial applications [4, 5]. Consequently, a thorough understanding of the fundamentals and properties of Si NWs is important [6, 7]. The challenges associated with comprehending the mechanical behavior of Si NWs underscore the need for a reliable testing method applicable to Si NWs, considering the complexities involved in their fabrication, testing, and characterization [4, 8–12]. Resonance testing, owing to its simplicity and successful outcomes, is commonly employed to acquire vibration modes and subsequently obtain mechanical properties [8, 13]. From a modeling perspective, atomistic simulations also offer a reliable approach for validating or examining the intrinsic effects in Si NWs [6, 14].

Exploring the mechanics of Si NWs offers an inclusive approach to material testing, providing substantial advantages in bridging the gap between theoretical methods and property assessments [6, 7, 15–17]. Additionally, by reducing the challenges associated with full-scale processing, it becomes feasible to seamlessly integrate materials characterization and property measurement [11]. In this context, the utilization of high-throughput and automated [7, 18, 19] testing techniques not only facilitates comprehensive data collection but also reveals deformation mechanisms essential for understanding the overall intrinsic properties of Si NWs [11]. Although conducting bending and resonance tests presents complex experimental challenges [6, 15, 20], the findings hold the potential to offer valuable insights into the intricacies of nano- and micro-scale structures, highlighting their importance as subjects of study. Given this perspective, investigating vibrational testing, with reference to successful cases in the literature, provides an opportunity to analyze fundamental properties such as modulus of elasticity of Si NWs [4, 16, 17, 21, 22]. It also facilitates comparisons of external influences, such as surface treatments or thermal processes, involved in the fabrication or assembly of nano-scale structures, particularly Si NWs within the framework of this study [23].

Understanding stress generation in nano- and micro-scale structures is crucial, not just from a theoretical standpoint, but also because the functionality of future MEMS and NEMS relies on comprehending the nature and intensity of stresses induced or generated during various fabrication, assembly, testing, or utilization stages [4, 6, 15]. In this context, Raman spectroscopy emerges as a widely employed technique for stress measurement in NWs, particularly in studies focusing on Si [24]. Raman analyses have shown stresses of up to 4 GPa and 1.2 GPa for highly strained silicon-on-insulator [25, 26] and stress-free substrates [6, 14, 15], respectively. This emphasizes the necessity for meticulous examination of any external influences, whether pre- or post-processing, given the significant impact of observed stress levels. Such scrutiny is essential, as these stresses can lead to variations of up to 85 GPa in the elastic properties of Si NWs [6].

While the resonance technique facilitates controlled testing, challenges arise in the fabrication of samples and the operation of the devices under test (DUTs), leading to a reduction in overall testing throughput. Recent studies suggest the potential for integrating fabrication and testing methodologies meticulously, allowing for the acquisition of numerous testing results for Si NWs fabricated within a single substrate [20]. This offers advantages for statistical analysis and the efficacy of the developed technique [20]. Nonetheless, further enhancements to testing and characterization methodologies necessitate a more systematic and interconnected approach, where the introduction of stresses to Si NWs can be accurately captured. Consequently, examining stresses and their subsequent effects on the mechanical properties of Si NWs becomes feasible from both theoretical and experimental perspectives.

The current investigation presents a comprehensive methodology for analyzing stresses induced in Si NWs through a systematic, interconnected approach involving thermal processes, Raman characterization, and resonance testing. The main aim is to establish a linked process for testing and characterizing Si NWs fabricated on stress-free substrates, while subjecting them to subsequent thermal steps to systematically introduce intrinsic stresses. Building upon prior successful studies by the authors, which focused on co-fabrication of Si NWs integrated into micro-scale support pillars [6, 15, 20, 27], characterization of surface- or fabrication-induced residual stresses [6, 14, 15], and high-throughput resonance testing of Si NWs, this research seeks to develop a methodology for introducing controlled stress and subsequently capturing it through follow-up testing and measurement assessments. This facilitates the analysis of vibrational modes and intrinsic stresses post-fabrication and after the thermal process, enabling precise induction and subsequent examination of thermal effects on Si NWs. Notably, the co-fabrication process for creating double-clamped Si NWs within a single substrate reduces sample-to-sample variations, enhancing the statistical robustness of the findings. For detailed insights into the fabrication method, testing procedure, Raman characterization, and thermal process, refer to Section 2. The outcomes of resonance testing and Raman characterization are presented in Section 3.

2. Materials and methods

This section introduces the integrated methodology for Raman characterization and resonance testing of Si NWs fabricated in a double-clamped configuration. Section 2.1 provides detailed information on the specific design and fabrication of Si NWs connected to the support pillars. Additionally, Section 2.2 provides details on the resonance testing method. Section 2.3 discusses Raman characterization for quantifying intrinsic stress in Si NWs, while Section 2.4 outlines the thermal process details, presenting the methodology for inducing stress into Si NWs.

2.1. Fabrication

The process of fabricating Si NWs begins with a double-side polished $< 100 >$ Si wafer, measuring 525 μm in thickness, which is diced into multiple fragments, each sized at 12 mm × 12 mm. The method involves masking a specific region of these fragments using a photoresist (PR) etch mask, followed by deep Si etching. This allows for the creation of suspended Si NW and its micro-scale accompanying support structures. To initiate the fabrication, the fragment undergoes a standard RCA1 cleaning process, after which a dielectric etch mask is applied via plasma-enhanced chemical vapor deposition. Subsequently, photolithography is employed to define the desired feature on the PR. Following the patterning of the dielectric etch mask, deep reactive ion etching (DRIE) is carried out to remove the Si beneath the etch mask [27]. This allows for the release of Si NWs upon etching process. Following this, O_2 ashing and selective vapor etching using hydrofluoric (HF) acid are performed to remove the protective layers, enabling precise definition of $< 110 >$-oriented Si NWs and micro-scale triangular supports within the substrate.

2.2. Resonance testing

The frequency response of Si NWs is examined using a Laser Doppler Vibrometer (LDV MSA-600, Polytec GmbH). The experimental setup entails placing the DUT onto a piezoelectric disk, secured with adhesive tape for actuation. Vibrational spectra are captured by activating the piezoelectric disk with a sinusoidal chirp signal generated by the LDV system within the specified frequency range. Subsequently, the device's response is analyzed using Fast Fourier Transform (FFT) techniques. The LDV is capable of generating an excitation signal ranging from 0 to 25 MHz, with 1.25 kHz increments, to drive the piezoelectric disk. This induces vibration in the sample positioned on top of the piezoelectric disk. A piezo-ceramic actuator

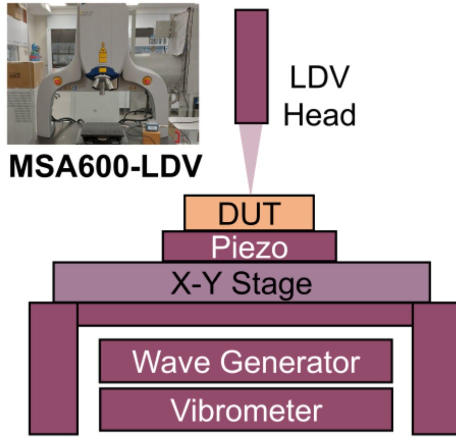

FIGURE 1. The experimental setup employs an LDV for conducting resonance tests on Si NWs. DUT refers to the Si fragment hosting Si NWs and accommodates specific scanning points assigned to both the Si NWs and support pillars, employing the MSA-LDV setup for resonance testing.

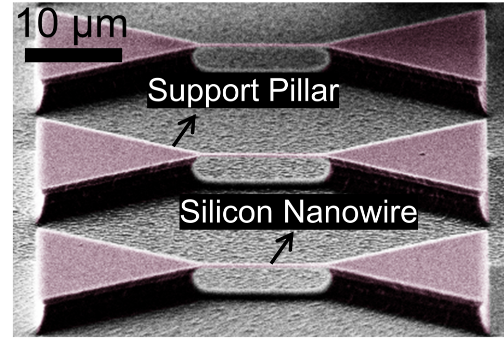

FIGURE 2. A array of Si NWs connected to triangular supports with an etch depth of 5 μm (achieved through the fabrication procedure detailed in Section 2.1), exhibiting consistent width, thickness, and length. The Si NWs measure 500 nm in thickness, 1000 nm in height, and 15 μm in length.

disk is utilized to produce high-frequency excitation via a periodic chirped signal. Figure 1 illustrates the testing setup and relevant details for conducting resonance tests on the DUT hosting multiple Si NWs. The scan points assigned using the MSA-LDV setup undergo resonance testing for comprehensive analysis [23].

2.3. RAMAN CHARACTERIZATION

After conducting dimensional analysis of Si NWs using sca nning electron microscope (SEM), Raman spectroscopy is employed to quantify the intrinsic stress, denoted as σ, using Equations 1 and 2:

$$\Delta\omega = \frac{1}{2\omega_0}\Big[[pS_{12} + q(S_{11} + S_{12})]\Big]\sigma = (SSC)\sigma, \quad (1)$$

$$\Delta\omega = -1.93 \times 10^{-9} \times (\sigma[Pa]), \quad (2)$$

where S_{11} and S_{12} are the elastic constants, p and q are the phonon deformation profiles. The stress shift coefficient (SSC) is calculate using $S_{11} = 7.68\times10^{-12}\,\mathrm{Pa}^{-1}$ and $S_{12} = -2.14 \times 10^{-12}\,\mathrm{Pa}^{-1}$ for quantifying the stress via Raman shift given as $\Delta\omega$ (ω_0 represents unstrained Si peak). To accomplish this, line scans are performed along both the Si NW and support pillars, with the latter serving as a reference for bulk measurement. The outcome of line scans for the support pillars and Si NW is used for the calculation of the Raman shift. A Lorentz model is applied to fit the Raman peaks of NWs under tension. Further details concerning the determination of stress induced by native oxide formation and comparative computational investigations can be found elsewhere [6, 14, 15].

2.4. THERMAL PROCESS

The thermal processing is conducted utilizing a Solaris 150 mm Rapid Thermal Process Oven. To guarantee temperature stability, preliminary processes are executed without the sample before the actual processing begins. Nitrogen gas is continuously introduced into the chamber throughout the process at a flow rate of 10 sccm. The sample is subjected to heating at 400 °C for 70 minutes, with an initial ramp rate of 150 °C sec^{-1} until the desired temperature is attained. The stress generated in Si NWs is anticipated due to the confined size of the nanostructures when subjected to heating in a double-clamped configuration [6, 14]. Its existence can be easily misinterpreted as an increase or reduction of resonator modulus of elasticity in the case of tensile or compressive stresses, respectively.

3. RESULTS

The results of the Si NWs fabrication process are detailed in Section 3.1. Furthermore, Section 3.2 presents discussions on Raman characterization and resonance testing outcomes.

3.1. FABRICATION OF SI NWS

The co-fabrication method employed for Si NWs enables the creation of multiple samples on a single chip, allowing for subsequent resonance testing following comprehensive structural and intrinsic stress characterizations conducted using SEM and Raman setups. This fabrication approach facilitates the production of Si NWs with consistent geometric and lithographic configurations on a single stress-free Si substrate, referred to as DUT, which in turn allows for detailed testing and characterization. As illustrated in Figure 2, Si NWs with uniform fabrication processes are produced in close proximity using the methodology outlined in Section 2.1. Here, the use of low-temperature processes and the ability to achieve multiple samples within a single fabrication process, incorporating MEMS-level structures as support pillars and NEMS-level features as Si NWs, are critical aspects of this methodology. Figure 2 showcases an array of Si NWs

with dimensions of 500 nm in thickness, 1000 nm in height, and 15 μm in length. These Si NW structures are co-fabricated with an etch depth of 5 μm, allowing for sufficient space for subsequent testing procedures. The developed process flow demonstrates notable repeatability, resulting in a high-yield process that facilitates the evaluation of Si NWs with desired dimensions. The fabrication technique eliminates the need for additional processes, ensuring that Si NWs can undergo deformations in different directions relative to the modal resonance state. Furthermore, each Si NW under examination undergoes SEM, resonance testing, and Raman analysis before the thermal processing step described in Section 2.4. Subsequently, these analyses are repeated after the thermal process is conducted to induce residual stress into the Si NWs, allowing for a thorough investigation of changes in Raman and resonance frequency shifts, which will be discussed in Section 3.2. Further details on the fabrication of such Si NWs can be found elsewhere [27].

3.2. Characterization and testing of Si NWs

Following the dimensional analysis of Si NWs, Raman spectroscopy is employed to quantify the intrinsic stress, denoted as σ, utilizing Equation 1 and Equation 2. Line scans are conducted along both the Si NW and support pillars, with the latter serving as a reference for bulk measurement. Figure 3a illustrates the results of these line scans, indicating Raman shifts of 520.24 cm^{-1} and 519.61 cm^{-1} for the support pillars and Si NW before the thermal process, respectively, resulting in a downshift of 0.62 cm^{-1}. The measurements are repeated on Si NWs once the thermal process is completed. Figure 3b illustrates the results of these line scans, indicating Raman shifts of 520.63 cm^{-1} and 517.14 cm^{-1} for the support pillars and Si NW after the thermal process, respectively, resulting in a downshift of 3.48 cm^{-1}. Given the obtained Raman shifts for the Si NW under investigation before and after thermal processing, Figure 4a and Figure 4b represent the shifts obtained along the NW longitudinal axis, depicting micropillar supports and Si NWs, before and after the thermal process, respectively. A Lorentz model is employed to fit the Raman peaks experiencing tensile stress before and after thermal processing with different magnitudes. The shift towards lower wavenumbers indicates a tensile intrinsic stress along the NW axis, with a tensile stress of 325 MPa and 1.8 GPa before and after thermal processing, respectively. In this respect, the standard deviation in stresses characterized before and after thermal processing are obtained for three Si NWs, resulting in 90.7 MPa and 265.3 MPa, respectively.

The resulting stress, induced by a thermal process and measured at 1.4 GPa, along with noticeable changes in Raman shifts as shown in Figure 3 and Figure 4, confirms the introduction of thermal effects into the double-clamped Si NW configuration. This also

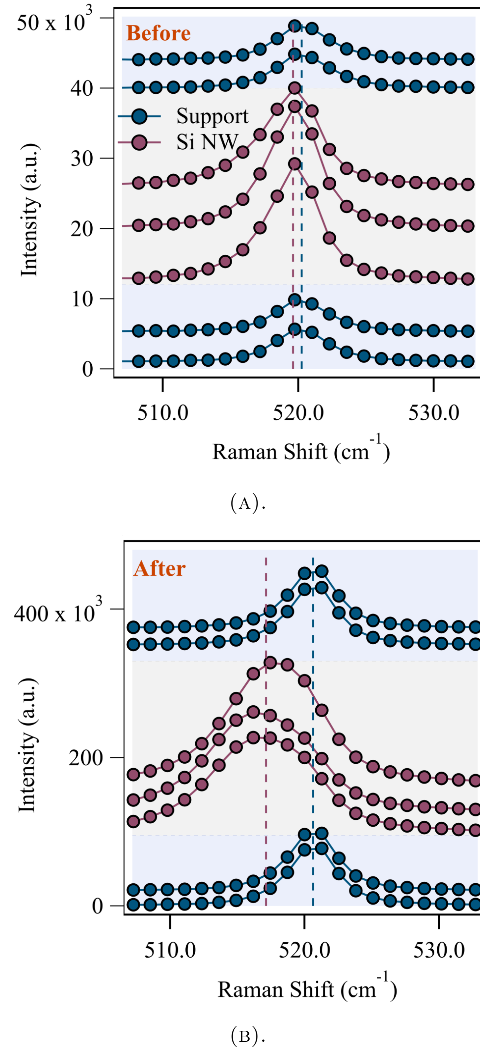

Figure 3. Raman spectra obtained via line scans conducted on suspended Si NWs and micro-scale supports (a) before and (b) after thermal processing. The averages associated with Raman shifts for Si NW and supports are given in dashed lines.

underscores the accurate calibration of the Raman analysis for detecting stresses present in the SiNWs under examination within this study. Furthermore, resonance testing will serve as the subsequent characterization method for a detailed investigation of the residual stress introduced into Si NWs through thermal processes. Further details regarding the determination of stress induced by native oxide formation and comparative computational investigations involving intrinsic stresses utilizing atomistic modeling can be found elsewhere [6, 14, 15]. The stress observed in this study is consistent with previously reported values for Si NWs, attributed to intrinsic or thermal processes, including thermal expansion mismatch between the Si and surface layer [6, 14]. The power calibration of Raman spectroscopy is employed to confirm that the stress values are not influenced by phase transitions or measurement artifacts, consistent with prior experimental findings [14, 25, 26].

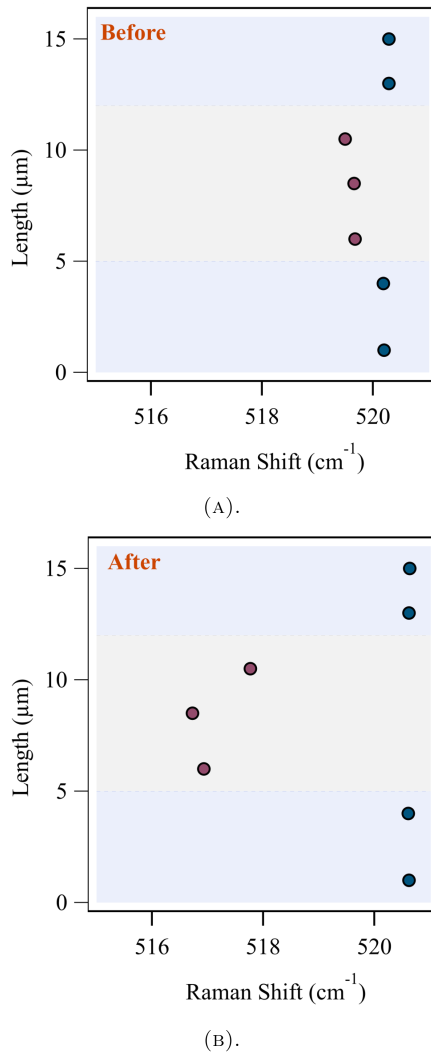

(A).

(B).

FIGURE 4. Raman shifts derived from the data in Figure 3, displayed along the Si NW (a) before and (b) after thermal processing. The blue and violet data points correspond to support and Si NW, respectively.

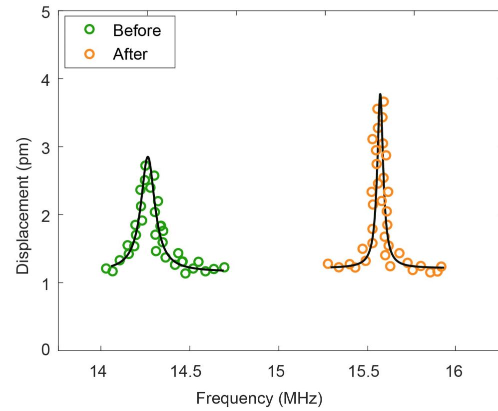

FIGURE 5. Displacement versus resonant frequency, along with Lorentzian fits, depicted for Si NW before and after thermal process. Resonance measurements indicate the occurrence of the first mode (out-of-plane) mechanical resonance at frequencies of 14.27 MHz and 15.57 MHz for the Si NW before and after thermal processing.

To perform resonance testing, the Si NW undergoes vibrational analysis following the methodology detailed in Section 2.2. The results, illustrating displacement versus frequency for the Si NW before and after thermal processing, are presented in Figure 5. Lorentzian fits are applied to illustrate the peaks observed in the responses, aiding in the identification of the first mode of resonance for Si NW. This approach yields resonance frequencies of 14.27 MHz and 15.57 MHz for the Si NW before and after thermal processing, respectively. Further calculations of the quality factor (Q-factor) [28] for Si NW reveal an increase from 37 to 117 for the Si NW before and after the thermal process, respectively. The observed shift in frequency response and Q-factor for the Si NW under examination offers another independent observation of the stresses introduced into Si NWs through the process outlined in Section 2.4.

In this context, the introduction of intrinsic stress into the Si NW under examination through thermal processing is investigated via Raman characterization and resonance testing. Both methodologies independently validate the shifts observed in Raman data and frequency responses. The results obtained herein offer a dependable methodology for extending the approach developed for examining multiple samples, facilitating detailed statistical analysis and precise investigation of intrinsic stresses and their subsequent impact on the behavior of Si NWs.

4. CONCLUSIONS

In conclusion, this paper emphasizes the complex interplay between intrinsic stress and mechanical behavior of Si NWs. Through a comprehensive examination utilizing techniques including Raman characterization, resonance testing, and thermal processing, the intrinsic stresses induced into Si NW under investigation is analyzed. The integration of these methodologies provides valuable insights into the mechanical properties of Si NWs and facilitates the development of a reliable testing methodology for streamlining the examination of multiple samples. These findings underscore the importance of understanding and controlling intrinsic stresses in Si NWs for the advancement of next-generation electronics.

ACKNOWLEDGEMENTS

S.Z.P., B.A. and B.E.A. gratefully acknowledge the financial support by Tubitak under grant no. 120E347 and 118C155. The authors acknowledge the use of the services and facilities of n^{2}STAR-Koç University Nanofabrication and Nanocharacterization Center for Scientific and Technological Advanced Research for the fabrication processes of this work. The authors acknowledge Dr. M Baris Yagci and Dr. Gülsu Şimşek Franci from Koç University Surface Technologies Research Center (KUYTAM) for the characterization steps of this work.

References

[1] S. Raman, R. Sankar, M. Sindhuja. Advances in silicon nanowire applications in energy generation, storage, sensing, and electronics: A review. *Nanotechnology* **34**(18):182001, 2023. https://doi.org/10.1088/1361-6528/acb320

[2] V. S. Vendamani, S. V. S. Nageswara Rao, A. P. Pathak, V. R. Soma. Silicon nanostructures for molecular sensing: a review. *ACS Applied Nano Materials* **5**(4):4550–4582, 2022. https://doi.org/10.1021/acsanm.1c04569

[3] S. A. Ahad, T. Kennedy, H. Geaney. Si nanowires: From model system to practical Li-Ion anode material and beyond. *ACS Energy Letters* **9**(4):1548–1561, 2024. https://doi.org/10.1021/acsenergylett.4c00262

[4] M. Nasr Esfahani, B. E. Alaca. A review on size-dependent mechanical properties of nanowires. *Advanced Engineering Materials* **21**(8):1900192, 2019. https://doi.org/10.1002/adem.201900192

[5] M. A. Darwish, W. Abd-Elaziem, A. Elsheikh, A. A. Zayed. Advancements in nanomaterials for nanosensors: A comprehensive review. *Nanoscale Advances* **6**(16):4015–4046, 2024. https://doi.org/10.1039/D4NA00214H

[6] S. Zare Pakzad, M. Nasr Esfahani, Z. Tasdemir, et al. Nanomechanical modeling of the bending response of silicon nanowires. *ACS Applied Nano Materials* **6**(17):15465–15478, 2023. https://doi.org/10.1021/acsanm.3c02077

[7] S. Z. Pakzad, M. N. Esfahani, B. E. Alaca. Investigation of the bending behavior in silicon nanowires: A nanomechanical modeling perspective. *International Journal of Applied Mechanics* **16**(07):2450073, 2024. https://doi.org/10.1142/S175882512450073X

[8] H. D. Espinosa, R. A. Bernal, T. Filleter. *In-situ* TEM electromechanical testing of nanowires and nanotubes. In *Nano and Cell Mechanics: Fundamentals and Frontiers*, pp. 191–226. Wiley Online Library, 2013. https://doi.org/10.1002/9781118482568.ch8

[9] C. Yang, E. Van Der Drift, P. French. Review of scaling effects on physical properties and practicalities of cantilever sensors. *Journal of Micromechanics and Microengineering* **32**(10):103002, 2022. https://doi.org/10.1088/1361-6439/ac8559

[10] G. Dehm, B. N. Jaya, R. Raghavan, C. Kirchlechner. Overview on micro- and nanomechanical testing: New insights in interface plasticity and fracture at small length scales. *Acta Materialia* **142**:248–282, 2018. https://doi.org/10.1016/j.actamat.2017.06.019

[11] D. S. Gianola, N. M. della Ventura, G. H. Balbus, et al. Advances and opportunities in high-throughput small-scale mechanical testing. *Current Opinion in Solid State and Materials Science* **27**(4):101090, 2023. https://doi.org/10.1016/j.cossms.2023.101090

[12] J. Xu, A. D. Refino, A. Delvallée, et al. Deep-reactive ion etching of silicon nanowire arrays at cryogenic temperatures. *Applied Physics Reviews* **11**(2):021411, 2024. https://doi.org/10.1063/5.0166284

[13] M. Elhebeary, M. T. A. Saif. Lessons learned from nanoscale specimens tested by mems-based apparatus. *Journal of Physics D: Applied Physics* **50**(24):243001, 2017. https://doi.org/10.1088/1361-6463/aa6e2b

[14] M. Nasr Esfahani, S. Zare Pakzad, T. Li, et al. Effect of native oxide on stress in silicon nanowires: Implications for nanoelectromechanical systems. *ACS Applied Nano Materials* **5**(9):13276–13285, 2022. https://doi.org/10.1021/acsanm.2c02983

[15] S. Zare Pakzad, M. Nasr Esfahani, Z. Tasdemir, et al. A new characterization approach to study the mechanical behavior of silicon nanowires. *Mrs Advances* **6**(19):500–505, 2021. https://doi.org/10.1557/s43580-021-00117-x

[16] S. Z. Pakzad, M. N. Esfahani, B. E. Alaca. The role of native oxide on the mechanical behavior of silicon nanowires. *Materials Today Communications* **34**:105002, 2023. https://doi.org/10.1016/j.mtcomm.2022.105002

[17] S. Z. Pakzad, M. N. Esfahani, B. E. Alaca. Mechanical properties of silicon nanowires with native oxide surface state. *Materials Today Communications* **38**:108321, 2024. https://doi.org/10.1016/j.mtcomm.2024.108321

[18] A. Barrios, C. Kunka, J. Nogan, et al. Automated high-throughput fatigue testing of freestanding thin films. *Small Methods* **7**(7):2201591, 2023. https://doi.org/10.1002/smtd.202201591

[19] D. Wang, W. Jiang, S. Li, et al. A comprehensive review on combinatorial film via high-throughput techniques. *Materials* **16**(20):6696, 2023. https://doi.org/10.3390/ma16206696

[20] S. Z. Pakzad, B. Ali, S. B. Coban, et al. Innovative MEMS stage for automated micromechanical testing. In *2023 International Conference on Manipulation, Automation and Robotics at Small Scales (MARSS)*, pp. 1–6. IEEE, 2023. https://doi.org/10.1109/MARSS58567.2023.10294157

[21] S. Z. Pakzad, M. N. Esfahani, B. E. Alaca. An analytical-atomistic model for elastic behavior of silicon nanowires. *Journal of Physics: Materials* **7**(3):03LT04, 2024. https://doi.org/10.1088/2515-7639/ad618d

[22] S. Z. Pakzad, M. N. Esfahani, B. E. Alaca. Molecular dynamics study of orientation-dependent tensile properties of si nanowires with native oxide: Surface stress and surface energy effects. In *2021 IEEE 21st International Conference on Nanotechnology (NANO)*, pp. 370–373. IEEE, 2021. https://doi.org/10.1109/NANO51122.2021.9514301

[23] S. Z. Pakzad, B. Ali, M. Muzammil, et al. High-throughput vibrational testing of silicon nanowires. In *2024 International Conference on Manipulation, Automation and Robotics at Small Scales (MARSS)*, pp. 1–6. IEEE, 2024. https://doi.org/10.1109/MARSS61851.2024.10612744

[24] S. J. Harris, A. E. O'neill, W. Yang, et al. Measurement of the state of stress in silicon with micro-Raman spectroscopy. *Journal of Applied Physics* **96**(12):7195–7201, 2004. https://doi.org/10.1063/1.1808244

[25] L. B. Spejo, J. L. Arrieta-Concha, M. Puydinger dos Santos, et al. Non-linear Raman shift-stress behavior in top-down fabricated highly strained silicon nanowires. *Journal of Applied Physics* **128**(4):045704, 2020. https://doi.org/10.1063/5.0013284

[26] R. A. Minamisawa, M. J. Süess, R. Spolenak, et al. Top-down fabricated silicon nanowires under tensile elastic strain up to 4.5%. *Nature communications* **3**(1):1096, 2012. https://doi.org/10.1038/ncomms2102

[27] S. Zare Pakzad, S. Akinci, M. Karimzadehkhouei, B. E. Alaca. Simplified top-down fabrication of sub-micron silicon nanowires. *Semiconductor Science and Technology* **38**(12):125005, 2023. https://doi.org/10.1088/1361-6641/ad0791

[28] D. A. Smith, V. C. Holmberg, D. C. Lee, B. A. Korgel. Young's modulus and size-dependent mechanical quality factor of nanoelectromechanical germanium nanowire resonators. *The Journal of Physical Chemistry C* **112**(29):10725–10729, 2008. https://doi.org/10.1021/jp8010487